Available online at www.sciencedirect.com
ScienceDirect
Thermochimica Acta 465 (2007) 73–82
thermochimica acta
www.elsevier.com/locate/tca

Kinetics of the thermal degradation of chitosan

Douglas de Britto, Sergio Paulo Campana-Filho *

Instituto de Química de São Carlos, Universidade de São Paulo, Av. trabalhador são-carlense, 400, 13560-970 São Carlos, SP, Brazil

Received 23 September 2005; received in revised form 26 September 2007; accepted 27 September 2007
Available online 2 October 2007

Abstract

The thermal degradation of chitosan, degree of acetylation 12%, was studied by using TG in nitrogen atmosphere in isothermal and dynamic conditions. Temperatures ranging from 240 °C to 280 °C were studied in isothermal conditions while heating rates in the interval 2.5–15.0 °C/min were employed when using dynamic conditions. The data issued from the dynamic experiments were treated by the methods proposed by Ozawa–Flynn–Wall and Kissinger, resulting in apparent activation energy of 149.6 kJ/mol and 138.5 kJ/mol, respectively. The approach proposed by MacCallum was used to treat the data issued from the isothermal experiments, resulting in E_a = 153 kJ/mol in good agreement with the results issued from the dynamic experiments. The use of the isoconvertional method due to Vyazovkin also showed a good agreement with the value of the activation energy issued by applying the method of Ozawa–Flynn–Wall. It was also observed that regardless of using isothermal or dynamic experimental conditions, the kinetic model best suited to describe the thermal degradation of chitosan is the catalytic Šesták–Berggren model.

Keywords: Chitosan; Thermal degradation; Activation energy; Šesták–Berggren model

1. Introduction

Chitosan is a linear copolymer composed of β(1 → 4)-linked 2-acetamido-2-deoxy-β-D-glucopyranose and 2-amino-2-deoxy-β-D-glucopyranose units. It occurs as a component of the cell wall of some fungi but it is generally produced by carrying out the deacetylation of chitin, an abundant polysaccharide found in the shells of crustaceans, particularly crabs and shrimps [1]. Due to its special physical chemical and biological properties chitosan has extensive applications in the food industry [2], agriculture [3], pharmacy and medicine [4,5] and waste water treatment [6]. Indeed, chitosan is a biocompatible and biodegradable polymer [7] whose degradation pathway has been studied by various methods [8–11]. In view of the new applications of this environmentally friendly polymer further studies shall be developed to determine its thermal stability as well as to allow a better understanding on the mechanistics and kinetics aspects involved in the thermal degradation of the polymer.

The thermogravimetric analysis has been widely used by many authors to investigate the kinetics of the thermal degradation of chitosan and derivatives. However, although the mathematical description of the decomposition process of polymers in the solid state rely on three kinetic components, namely the two Arrhenius parameters, apparent activation energy (E_a) and pre-exponential factor (A), and the analytical expression describing the kinetic model, $f(\alpha)$, the former parameter (E_a) is the most frequently used to discuss the thermal stability of these polymers. Isothermal and dynamic conditions and many different methods have been employed to determine the apparent activation energy of the thermal decomposition of chitosan and derivatives, as films or powders, in nitrogen or air atmosphere. Thus, a comparison among these studies is not always easy to be done due to the different conditions employed and sometimes the incomplete characterization of the polymers makes it still more difficult. Cárdenas et al. [12] reported E_a = 71 kJ/mol by applying dynamic conditions to study the thermal degradation of chitosan while Peniche-Covas et al. [13] carried out their study in dynamic and isothermal conditions and they found E_a = 181 kJ/mol and E_a = 183–227 kJ/mol, respectively. Both studies were carried out in nitrogen atmosphere, but the average degree of acetylation ($\overline{DA}$), an important characteristic of chitosan, is not reported in the former study while a

* Corresponding author. Fax: +55 1633739952.
E-mail address: scampana@iqsc.usp.br (S.P. Campana-Filho).

0040-6031/$ – see front matter © 2007 Elsevier B.V. All rights reserved.
doi:10.1016/j.tca.2007.09.008

sample having $\overline{DA}$ = 10% was used in the latter work. The former authors also studied a set of acylated derivatives of chitosan and they found that the E_a values ranged from 41 kJ/mol to 170 kJ/mol depending on the acyl substituent, while the latter authors reported that the mercaptyl derivative of chitosan presented slightly smaller E_a values as compared to the parent chitosan. However, no mention is made on the influence of the degree of substitution of these chitosan derivatives on their thermal degradation. Qu et al. [14] reported E_a = 113 kJ/mol and E_a = 157–160 kJ/mol for the thermal degradation of chitosan ($\overline{DA}$ = 12%) in dynamic and isothermal conditions, respectively, while its polyesters derivatives presented smaller E_a values independently of the thermal condition employed to study its degradation. The thermal degradation of these derivatives also showed a dependence of E_a on the average degree of substitution and on the chemical nature of the side chains. More recent studies reported E_a = 147–166 kJ/mol [15] and E_a = 82 kJ/mol [16] when the thermal degradation of chitosan was studied in dynamic conditions and E_a = 138–158 kJ/mol [16] in isothermal conditions. Both studies were carried out in nitrogen atmosphere and employed chitosan of $\overline{DA}$ = 22%. In the latter case, *N*,*N*,*N*-trimethylchitosan derivatives of varying degrees of quaternization were also studied, their activation energies determined in isothermal conditions being roughly twice those issued from the dynamic study. In this latter study it was also found that the activation energy of the methylated derivatives was higher than that of the parent chitosan and that it decreased as the degree of methylation increased [16].

These data reveal a general lack of agreement among the different studies concerning the E_a values determined in dynamic and isothermal conditions and it should also be noted that the kinetic model for the thermal decomposition was not determined, the assumption of a first-order process with $f(\alpha) = (1 - \alpha)$ being generally adopted.

In this work the values of E_a for the first stage of the thermal decomposition of chitosan are determined by applying different approachs and by studying it in dynamic and isothermal conditions. A comparison among these methods is established and the test proposed by Málek et al. [17] is applied to determine which kinetic model is best suited to describe the thermal decomposition of chitosan.

2. Experimental

Commercial chitosan (high molecular weight chitosan from crab shells, by Fluka/Biochimica) was purified by suspending 1 g of the polysaccharide in 0.3 dm^{-3} of 1 M lactic acid aqueous solution and stirring it overnight. The resulting solution was filtered through 5.0 μm mixed cellulose ester membrane filter (Millipore) to eliminate insoluble matter and the chitosan was precipitated upon the addition of a concentrated NH_4OH aqueous solution. Following the extensive washing with water, the precipitate was extensively washed with methanol and dried at ambient conditions. Then it was milled in a domestic blender and the fraction of particles having an average diameter lower than 125 μm was used for the analyses. The purified chitosan was characterized by ^{1}H NMR and infrared spectroscopy as described elsewhere [16].

The dynamic and isothermal degradation studies were carried out by using 4–5 mg of the purified chitosan in nitrogen atmosphere (gas flow of 0.050 dm^{-3}/min) in a TGA50 SHIMADZU thermal analyzer.

For the dynamic experiments the samples were heated from room temperature to 500 °C at a heating rate varying from 2.5 °C/min to 15.0 °C/min while the loss of mass was monitored. For the isothermal experiments the samples were heated at a rate of 10 °C/min to 150 °C, maintained at this temperature for 10 min and then heated at a rate of 20 °C/min to the desired temperature. The zero time for the thermal degradation study was taken in the moment at which the temperature stabilized.

3. Theoretical background

3.1. The kinetic parameters

The kinetic analysis of a thermal degradation process shall begin by expressing the reaction rate by a general equation such that [18]:

$$\frac{d\alpha}{dt} = k(T) f(\alpha) \tag{1}$$

where t represents the time, α is the extent of reaction, T is the temperature, $k(T)$ is the temperature-dependent rate constant and $f(\alpha)$ is a temperature-independent function that represents the reaction model. The rate constant $k(T)$ is given, generally, by the Arrhenius equation:

$$k(T) = A \exp\left(-\frac{E_a}{RT}\right) \tag{2}$$

where A is the pre-exponential or frequency factor and E_a is the apparent activation energy. Thus, Eq. (1) may be rewritten as:

$$\frac{d\alpha}{dt} = A \exp\left(-\frac{E_a}{RT}\right) f(\alpha) \tag{3}$$

The integration of Eq. (3) allows the determination of E_a, as proposed by Vyazovkin and Wight [18] and by MacCallum [19], by using:

$$\frac{E_a}{RT} + \ln[g(\alpha)] - \ln A = \ln t \tag{4}$$

where $g(\alpha)$ results from the integration of $f(\alpha)$.

Thus, several isothermal experiments may be carried out and the logarithm of the time taken to reach a fixed extent of conversion, α, plotted against the reciprocal of the temperature of the experiment will yield the straight line whose slope is E_a/R.

If the temperature is changed with the time ($\beta = dT/dt$) as occurs in dynamic experiments, the Eq. (3) assumes the form:

$$\frac{d\alpha}{dT} = \frac{A}{\beta} \exp\left(-\frac{E_a}{RT}\right) f(\alpha) \tag{5}$$

The integration of Eq. (5) results:

$$g(\alpha) = \frac{A}{\beta}\int_{T_0}^{T} \exp\left(-\frac{E_a}{RT}\right) dT = \frac{A}{\beta} I(E_a, T) \quad (6)$$

One of the major concerns about the Eq. (6) is that the temperature integral, $I(E_a, T)$, does not have an analytical solution. Indeed, only approximation solutions are proposed [20] such as the isoconversional method proposed by Ozawa–Flynn–Wall [21], which uses the Doyle approximation [22] and is expressed by:

$$\log \beta = \log \frac{AE_a}{g(\alpha)R} - 2.315\frac{0.4567E_a}{RT} \quad (7)$$

Therefore, if a set of experiments is run at different heating rates, β, then the value of E_a can be obtained from the plot of $\log \beta$ against $1/T$ for a fixed degree of conversion, the frequency factor, A, being determined by [23]:

$$A = \frac{\beta E_a}{RT_m^2} \exp\left(\frac{E_a}{RT_m}\right) \quad (8)$$

where T_m is the temperature of the maximum reaction rate.

The method proposed by Kissinger [24] relies on experiments carried out at different heating rates, β, and is expressed by:

$$\ln \frac{\beta}{T_m^2} = \left\{\ln \frac{AR}{E_a} + \ln[n(1-\alpha_p)^{n-1}]\right\} - \frac{E_a}{RT_m} \quad (9)$$

where α_p is the maximum conversion and n is the reaction order. Thus, the plot of $\ln \beta/T_m^2$ versus $1/T_m$ will yield the straight line whose slope is E_a/R.

3.2. The kinetic model

Once the apparent activation energy has been determined it is possible to find the kinetic model which corresponds to the better description of the experimental data issued from the TG experiments. For this purpose, it is possible to define two especial functions which can easily be obtained by transformation of experimental data [17,25]. For isothermal experiments these functions are:

$$Z(\alpha) = \left(\frac{d\alpha}{dt}\right) t = f(\alpha)g(\alpha) \quad (10)$$

$$Y(\alpha) = \left(\frac{d\alpha}{dt}\right) \approx f(\alpha) \quad (11)$$

The value of α at the maximum of the $Z(\alpha)$, α_Z^*, is characteristic of the kinetic model, the shape of the $Y(\alpha)$ function is formally identical to the kinetic model $f(\alpha)$ and its maximum value is labeled as α_Y^*.

Similarly, for dynamic conditions these functions, which have the same mathematical properties as those for isothermal conditions, are defined as:

$$Z(\alpha) \approx \left(\frac{d\alpha}{dT}\right) T^2 = f(\alpha)g(\alpha) \quad (12)$$

$$Y(\alpha) = \left(\frac{d\alpha}{dT}\right) \exp\left(\frac{E_a}{RT}\right) = Af(\alpha) \quad (13)$$

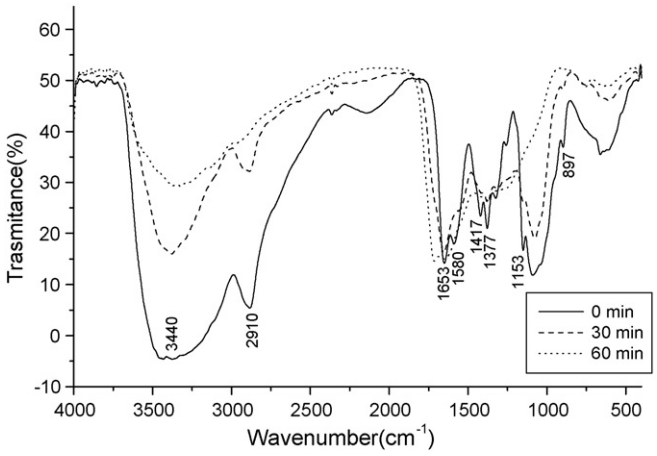

Fig. 1. Infrared spectrum of a chitosan film before and after heating it 280 °C for 30 min and 60 min in nitrogen atmosphere.

4. Results and discussion

4.1. Spectral characterization and evidences of the degradation of chitosan

The average degree of acetylation ($\overline{DA}$), an important characteristic of chitosan, may be determined by various techniques such as titrimetry, elemental analysis, thermogravimetric analysis, differential scanning calorimetry and infrared spectroscopy; however the NMR spectroscopy furnishes the most reliable results. In this work the average degree of acetylation of chitosan was determined from its ^{1}H NMR spectrum. Thus, according to the literature [26], the ratio of the intensities of the signals at $\delta = 1.99$, due to the hydrogen atoms of the methyl moieties of the acetamido groups, and at $\delta = 3.18$, attributed to the hydrogen atom bonded to the carbon 2 of the glycopiranose ring, allowed the determination of $\overline{DA} = 12\%$.

The most characteristic bands in the infrared spectrum of chitosan (Fig. 1) are [16,27,28]: (a) the strong and broad band centered at 3440 cm^{-1} which is attributed to the axial stretching of O–H and N–H bonds; (b) the band corresponding to the axial stretching of C–H bonds which is centered at 2910 cm^{-1}; (c) the bands centered at 1653 cm^{-1} and 1580 cm^{-1}, corresponding to the amide I and amide II vibrations, respectively; (d) the bands at 1417 cm^{-1} and 1377 cm^{-1} resulting from the coupling of C–N axial stretching and N–H angular deformation; (e) the bands in the range 1153–897 cm^{-1} due to polysaccharide skeleton, including the glycosidic bonds, C–O and C–O–C stretchings.

Fig. 1 also shows the spectra of chitosan after heating it at 280 °C for 30 min and 60 min in nitrogen atmosphere. The spectral changes are clearly seen, indicating the degradation of the polymer as a consequence of its heating. Thus, the decrease of the intensities of the bands listed above, particularly those at 3440 cm^{-1}, 2910 cm^{-1}, 1417 cm^{-1}, 1377 cm^{-1}, and in the range 1153–897 cm^{-1}, is attributed to dehydratation, deacetylation and depolymerization reactions. The deacetylation of chitosan should also result in the decrease of the bands at 1653 cm^{-1} and 1580 cm^{-1} but it is masked by the occurrence of intense bands at 1710–1500 cm^{-1}, which are attributed to

unsaturated structures formed during the degradation of chitosan [13,14,16].

As a consequence of the above-mentioned degradation reactions the thermally treated samples become brownish and insoluble in the usual solvents of chitosan, such as dilute aqueous solutions of acetic acid and hydrochloric acid. Therefore it was not possible to follow the degradation kinetics by ^{1}H NMR spectroscopy, however the infrared spectroscopy allowed the monitoring of the degradation reaction and gave some insight on the kinetic model, as will be discussed in Section 4.3.2.

4.2. The apparent activation energy and frequency factor

4.2.1. Dynamic experiments

The TG curves of chitosan scanned at different heating rates (β) from room temperature to 500 °C, in nitrogen atmosphere, are shown in Fig. 2 while the corresponding DTG curves in the range 200–400 °C are shown in the insert.

The TG curves show a first thermal event in the range 25–140 °C, which corresponds to a weight loss of approximately 6% and it is attributed to the evaporation of water loosely bound to the polymer; the second thermal event occurring in the range 200–400 °C is attributed to further dehydratation, to deacetylation and depolymerization of chitosan; the third event, for temperature higher than 400 °C, corresponds to the residual decomposition reactions [16]. The scope of this work will be focused on the first stage of the thermal degradation occurring after the initial dehydratation step, i.e. that one which occurs in the range 200–400 °C.

It is noted that the curves are shifted to higher temperatures as the heating rate increases from 2.5 °C/min to 15.0 °C/min (Fig. 2), this effect being more easily observed in the insert (DTG curves). Thus, the temperature corresponding to the maximum reaction rate, T_m, for the first stage of the thermal degradation of chitosan was determined from the DTG curves as being 294.3 °C, 305.0 °C, 318.9 °C and 328.6 °C for heating rates corresponding to 2.5 °C/min, 5.0 °C/min, 10.0 °C/min and 15.0 °C/min, respectively.

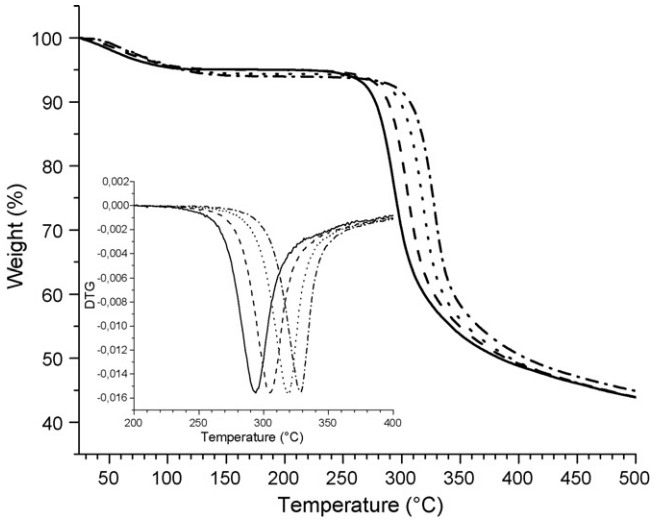

Fig. 2. TG curves of chitosan in the range 25–500 °C in nitrogen atmosphere for the following values of heating rate: β = 2.5 °C/min (—); β = 5.0 °C/min (- - -); β = 10.0 °C/min (· · ·); β = 15.0 °C/min (- · - · -). Insert: Corresponding DTG curves of chitosan in the range 200–400 °C.

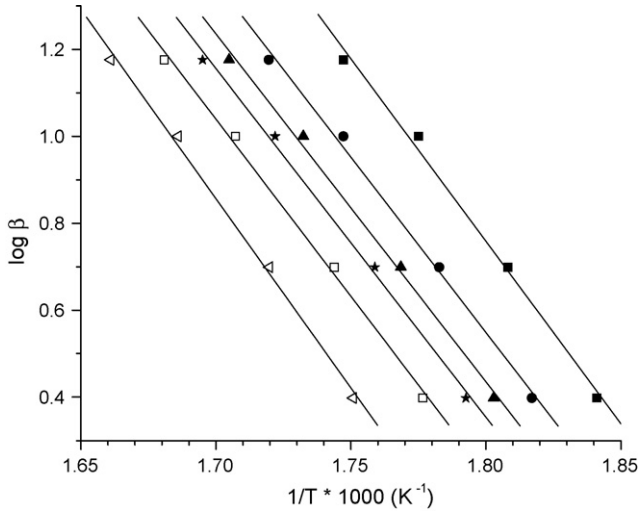

Fig. 3. Plots of log β versus 1000/T for the thermal degradation of chitosan at extents of conversion: α = 0.05 (■); α = 0.1 (●); α = 0.15 (▲); α = 0.2 (★); α = 0.3 (□); α = 0.5 (◁).

Following, the apparent activation energy and frequency factor of the first stage of the thermal degradation of chitosan were determined by treating the data issued from the dynamic experiments (Fig. 2) according to the methods proposed by Ozawa–Flynn–Wall [21] and Kissinger [24].

To apply the isoconversional method proposed by Ozawa–Flynn–Wall [21] to the first stage of the thermal degradation of chitosan scanned at different heating rates, the extensions of conversion α = 0 and α = 1 were taken at 200 °C and 400 °C, respectively. Although such extensions of conversion should vary at different temperature under different heating rate it is a valid estimate in the range of heating rate used in this study as all curves are approximately coincident at 200 °C and 400 °C regardless of the heating rate (Fig. 2). Thus, the curves log β versus 1/T were plotted for experimental data in the range $0.05 < \alpha < 0.5$ (Fig. 3), allowing the determination of the kinetic parameters E_a and A (Table 1).

Table 1
The Arrhenius parameters E_a and A, for the first stage of the thermal degradation of chitosan determined according to the method proposed by Ozawa–Flynn–Wall [21]

α	E_a (kJ/mol)	A (min^{-1})[a]	r
0.05	152.7	1.52×10^{13}	0.9971
0.1	146.8	1.59×10^{13}	0.9980
0.15	145.6	1.42×10^{13}	0.9982
0.2	145.9	8.31×10^{12}	0.9982
0.3	148.3	–	0.9982
0.5	158.4	–	0.9981
Average	149.6 ± 5.0	$1.34 \times 10^{13} \pm 7.1 \times 10^{12}$	

[a] Calculated from Eq. (8), for β = 2.5 °C/min, 5.0 °C/min, 10.0 °C/min and 15.0 °C/min from the top to the bottom of the column.

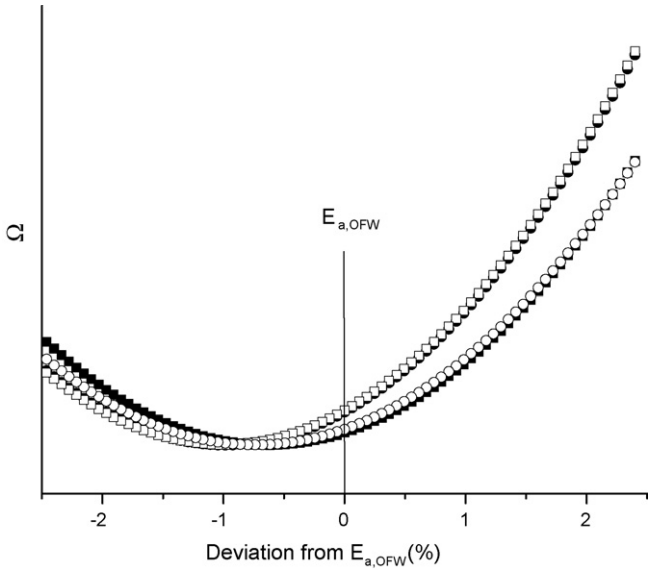

Fig. 4. Plots of Ω function versus deviation from the value of E_a calculated according Ozawa–Flynn–Wall method ($E_{a,OFW}$) at extents of conversion: $\alpha = 0.05$ (■); $\alpha = 0.15$ (●); $\alpha = 0.2$ (□) and $\alpha = 0.5$ (σ).

Vyazovkin proposed a new isoconvertional method which makes use of a more accurate approximation for the temperature integral [18,29]. According to this method, for a given set of experiments carried out at different heating rates, the activation energy can be determined at any particular extent of conversion by finding the value of E_a for which the function Ω (Eq. (14)) attains a minimum.

$$\Omega = \sum_{i}^{n} \sum_{j \neq i}^{i} \frac{I(E_{a\alpha}, T_{\alpha,i})\beta_j}{I(E_{a\alpha}, T_{\alpha,j})\beta_i} \quad (14)$$

where the subscript i and j represent experiments conducted at heating rate β_i and β_j, respectively.

The value of E_a determined by applying the approach due to Ozawa–Flynn–Wall was taking as a first approximation of the apparent activation energy ($E_{a,OFW}$) and the non isothermal data of the thermal degradation of chitosan were tested in the function Ω. In this way, the value of $E_{a,OFW}$ was increased and decreased steeply and these values were tested in the function Ω showing deviations smaller than 1% (Fig. 4). Such a small deviation was reported early [30,31] allowing one to conclude for the adequacy of a given approach to determine the apparent activation energy of the thermal degradation in the solid state. Thus, taking into account that the thermal degradation of chitosan is a complex process in which the variation of the apparent activation energy for different extension of reaction (α) is much greater than 1%, it is concluded that the treatment proposed by Ozawa–Flynn–Wall gave an acceptable approximation for the E_a.

By plotting $\ln \beta/T_m^2$ versus $1000/T_m$ (Fig. 5), as proposed by Kissinger [24], the apparent activation energy was determined from the slope of the resulting straight line as $E_a = 138.5$ kJ/mol, the values of the frequency factor corresponding to different heating rates being shown in Table 2.

An old method for determination of E_a, frequently applied to study the thermal degradation of chitosan [12–16], is the approach of Broido [32]. The major concern about this method is that it is based in a single heating rate experiment and it assumes a first order process or $f(\alpha) = (1 - \alpha)$. Only for comparison, the dynamic data were treated by this method giving $E_a = 143.0 \pm 2.5$ kJ/mol, a value which is very close to the average value found by applying the method of Ozawa–Flynn–Wall. On the other hand, the values of the frequency factor calculated by applying the method of Broido did not agree as well (6.33×10^{11} min^{-1}). Bearing in mind the strong limitations of this method, no further comments will be added and the eventual agreement of these results with others reported in here are taken as simple coincidence.

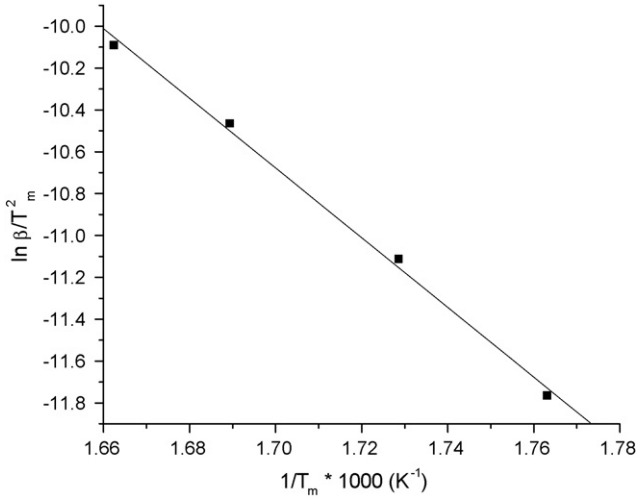

Fig. 5. Plot of $\ln \beta/T_m^2$ versus $1000/T_m$ for the thermal degradation of chitosan.

4.2.2. Isothermal experiments

In the isothermal experiments, the chitosan was heated to a temperature close to the onset of the first stage of its thermal degradation and it was maintained at this temperature for a given time while the loss of weight was monitored, allowing the calculation of the extension of conversion as a function of the reaction time. To allow an easier comparison of the results of the isothermal experiments with those issued from the dynamic ones, the extension of conversion of the former were normalized with respect to the maximum extension of conversion attained in the dynamic experiments. After normalization the experimental data were then treated according to the approach proposed by MacCallum [19]. The curves showing the plots of $\ln t$ versus $1/T$

Table 2
Frequency factor, A, determined by applying the approach of Kissinger [24]

β (°C/min)	α_p	A (min^{-1})
2.5	0.41	7.10×10^{11}
5.0	0.42	7.48×10^{11}
10.0	0.47	6.39×10^{11}
15.0	0.49	5.11×10^{11}
Average	–	$6.51 \times 10^{11} \pm 1.0 \times 10^{11}$

The values of A were calculated by taking into account the reaction order, n, expressed in Table 6.

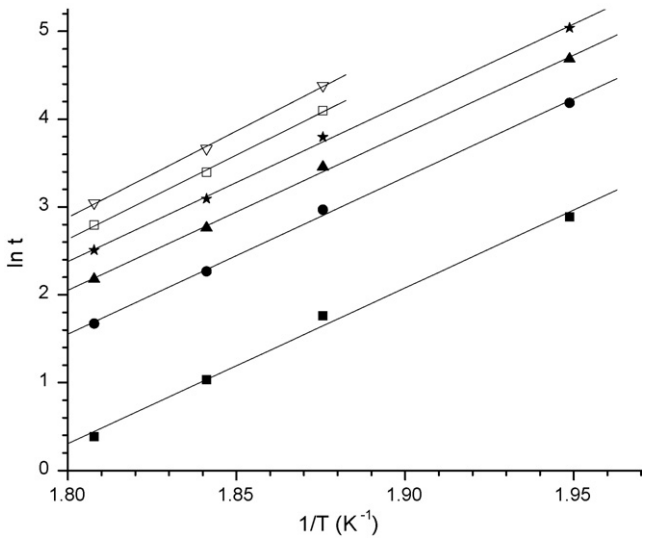

Fig. 6. Plots of ln t versus $1/T$ for the isothermal degradation of chitosan as a function of the extension of conversion: $\alpha = 0.02$ (■); $\alpha = 0.1$ (●); $\alpha = 0.2$ (▲); $\alpha = 0.3$ (⋆); $\alpha = 0.4$ (□); $\alpha = 0.5$ (▽).

as a function of the extension of conversion are seen in Fig. 6, while the values of E_a and A are listed in Table 3.

4.2.3. A survey of arrhenius parameters for the thermal degradation of chitosan

As already mentioned, the literature concerning the thermal degradation of chitosan reports, with some few exceptions such as the results reported in reference [13], the disagreement among the values of E_a determined by applying isothermal and dynamic methods. Also, very few works report on the values of the frequency factor. A comparison among some data reported in the literature and those determined in this work are shown in Table 4.

All the studies listed in Table 4 were carried out in nitrogen atmosphere with powdered chitosan except for that one reported in reference [16], in which films of chitosan were used, and that of reference [15], which employed an air atmosphere.

Concerning the results of this study, a good agreement is observed among the values of frequency factor which were determined from dynamic studies, mainly between those issued from the methods proposed by Broido and Kissinger but that one derived from Ozawa–Flynn–Wall's approach is higher than the former two. The other values of frequency factor which were also determined by applying dynamic methods are due to Cárdenas et al. [12] and Hong et al. [33], the former being several orders lower than anyone listed in Table 4 while the latter is close to those determined in this study. The highest value of the frequency factor is that one issued from this study which applied an isothermal method and the approach of MacCallum [19].

Table 3
Apparent activation energy, E_a, and frequency factor, A, for the isothermal degradation of chitosan determined according to the method proposed by MacCallum [19]

α	E_a (kJ/mol)	A (min^{-1})[a]	r
0.02	147.8	2.85×10^{14}	0.9970
0.1	148.6	1.33×10^{14}	0.9991
0.2	148.5	8.14×10^{13}	0.9994
0.3	150.0	–	0.9994
0.4	159.4	–	0.9993
0.5	164.0	–	0.9994
Average	153.0 ± 6.9	$1.66 \times 10^{14} \pm 1.0 \times 10^{14}$	

[a] Calculated from Eq. (16), for $T = 260\,^{\circ}C$, 270 °C and 280 °C from the top to the bottom of the column.

A possible explication for these divergences may be the different mathematical approximations used to treat the experimental data issued from the dynamic and isothermal methods. Indeed, a kinetic study on the thermal degradation of epoxy-anhydride resins also reported the disagreement concerning the determination of the frequency factor and apparent activation energy by isothermal and dynamic methods [25].

Recently, Gao et al. [34] reported an assessment on error of the pre-exponential factor estimated from the isoconversional plot of dynamic thermogravimetric measurements. Such a work pointed out that the error, close to −10% in the value of the pre-exponential factor, is closely related to the mathematical equations employed for its determination. As expressed in Eq. (7), the pre-exponential factor is derived from the intercept of the straight line resulting from the plot log β versus $1/T$. Thus, as the logarithm form is implied, even small deviations of the value of the intercept provoke large variations in the value of the pre-exponential factor. On the other hand, the activation energy is determined from the slope of the straight line and its variation is much less important than that of the pre-exponential factor.

According to the results of this work, the activation energy for the thermal degradation of chitosan seems to be slightly dependent on the method, dynamic or isothermal, employed for its determination. Indeed, our results present a good agreement among the values of E_a determined by both methods with the value determined from the isothermal experiment being approximately 10% higher than the lowest one determined by a dynamic experiment. However, Peniche-Covas et al. [13] and Qu et al. [14] reported values of E_a issued from the isothermal experiments which were, respectively, 20% and 28% higher than those determined by the dynamic experiments. Nevertheless, our results as well as those of these two latter studies show the same trend of increasing E_a as the extent of conversion increases during the isothermal experiments, suggesting the occurrence of complex reactions at the latter stages of the thermal degradation of chitosan [13,14].

On the other hand, the influence of the average degree of acetylation and physical form of the polymer, as well as of the atmosphere used to study the thermal degradation of chitosan, on the kinetic parameters cannot be evaluated by the data showed in Table 4. Indeed, the available data do not include a range sufficiently large of $\overline{DA}$ neither enough data on the thermal degradation of chitosan in different physical forms and atmospheres, but it seems reasonable to expect some influence of these factors on the thermal decomposition of chitosan. Thus, the availability of oxygen may be responsible for the occurrence of oxidative processes during the thermal degradation of chitosan, affecting the reaction mechanism and kinetic parameters. Also, the studies being currently developed in our laboratories show that powdered chitosan degrades faster than a film of chi-

Table 4
Values of apparent activation energy, E_a, and frequency factor, A, for the thermal degradation of chitosan

DA (%)	Atmosphere	Method	E_a (kJ/mol)	ln A	Ref.
22	N_2	Dynamic	82.1[a]	–	[16]
22	N_2	Isothermal	145.4[a]	–	[16]
12	N_2	Dynamic[b]	143.0	27.2 ± 0.4	This work
12	N_2	Dynamic[c]	149.6	30.2 ± 0.5	This work
12	N_2	Dynamic[d]	138.5	27.2 ± 0.1	This work
12	N_2	Isothermal[e]	153.0	32.7 ± 0.5	This work
12	N_2	Dynamic	113.0	–	[14]
12	N_2	Isothermal	156.8	–	[14]
–	N_2	Dynamic[f]	70.9	5.8	[12]
10	N_2	Dynamic	181.0	–	[13]
10	N_2	Isothermal	183–227	–	[13]
22	Air	Dynamic	147–166	–	[15]
16	N_2	Dynamic	140–160	28.1	[33]

[a] Experiments carried out with chitosan films.
[b] Broido's method.
[c] Ozawa–Flynn–Wall's method.
[d] Kissinger's method.
[e] MacCallum's method.
[f] In s^{-1}.

tosan, an effect attributed to the higher superficial area available in the former case, and that the activation energy is lower for the more deacetylated chitosans, suggesting an important role for the acetamido groups on the thermal degradation of chitosan.

4.3. The kinetic model

As our experimental data allow the calculation of the activation energy of the thermal degradation of chitosan from isothermal and dynamic experiments carried out in different temperatures and with diverse heating rates, respectively, the most probable kinetic model can be determined and compared to the experimental curves.

4.3.1. Isothermal experiments

The procedure proposed by Málek et al. [17,25] was used, from Eqs. (10) and (11), to determine the kinetic model best fitted to the experimental data of the isothermal degradation of chitosan resulting in the curves shown in Fig. 7.

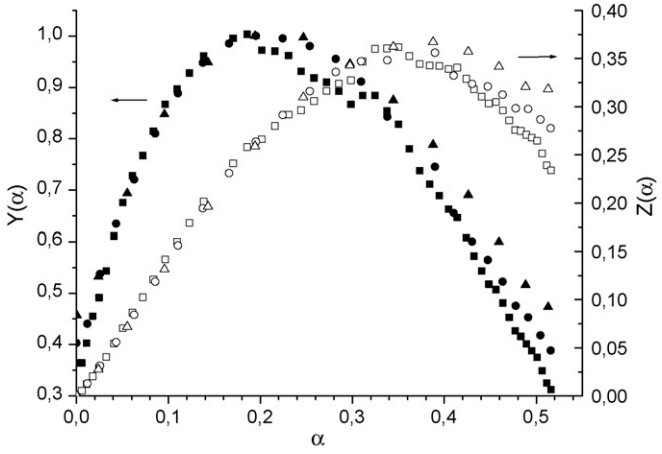

Fig. 7. The functions $Y(\alpha)$ (closed symbols) and $Z(\alpha)$ (open symbols) for the isothermal degradation of chitosan at 260 °C (□, ■); 270 °C (◯, ●); 280°C (Δ, ▲).

It is observed that the curves have approximately the same profile regardless of the temperature except for that corresponding to 240 °C (data not show). In this latter case no maximum for the dα/dt curve was observed, probably because the extension of conversion attained in this case is too low.

From the curves shown in Fig. 7 the maxima of the functions $Z(\alpha)$ and $Y(\alpha)$ were determined as $\alpha_Z^* = 0.37$ and $\alpha_Y^* = 0.22$, respectively. Thus, as $0 < \alpha_Y^* < \alpha_Z^*$, the catalytic SB model proposed by Sesták–Berggren [35], in which $f(\alpha) = \alpha^m(1-\alpha)^n$, seems to be the best fitted one. The exponents m and n of the kinetic expression for $f(\alpha)$ are given [17] by $p = m/n$, with p being expressed as:

$$p = \frac{\alpha_Y^*}{1-\alpha_Y^*} \tag{15}$$

Thus, the Eq. (3) can be rewritten as:

$$\ln\left[\frac{d\alpha}{dt}\exp\left(-\frac{E_a}{RT}\right)\right] = \ln A + n\ln[\alpha^p(1-\alpha)] \tag{16}$$

The plot of $\ln[(d\alpha/dt)\exp(E/RT)]$ versus $\ln[\alpha^p(1-\alpha)]$ for $0.2 < \alpha < 0.8$ results in a straight line whose angular and linear coefficients correspond to the exponent n and to ln A, respectively, the exponent m resulting from $m = pn$. The resulting values of m and n (Table 5) tend to decrease with increasing temperature.

Table 5
Values of the kinetic exponents m and n for the isothermal degradation of chitosan

T (°C)	m	n
260	1.35	4.82
270	1.11	3.98
280	0.93	3.31

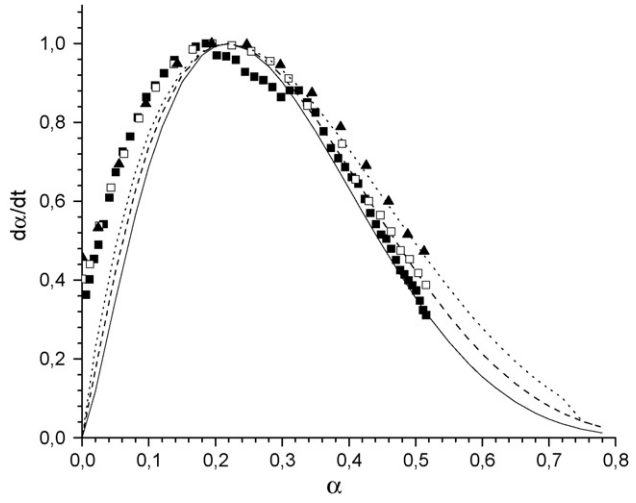

Fig. 8. Experimental (symbols) and simulated (lines) curves dα/dt versus α for the isothermal degradation of chitosan at temperature 260 °C (■) experimental/(—) simulated; 270 °C (□) experimental/(- - -) simulated; 280 °C (▲) experimental/(· · ·) simulated.

Thus, knowing the values of E_a and A and having a expression for $f(\alpha)$, it is possible to simulate the curve dα/dt which, after normalization, may correspond to the experimental curve dα/dt. The simulated and the experimental curves corresponding to the isothermal degradation of chitosan at 260 °C, 270 °C and 280 °C show a good agreement in the range of extension of conversion attained in our experiments (Fig. 8), indicating that the kinetic parameters and the expression of $f(\alpha)$ adopted for the simulation are quite suitable.

4.3.2. Dynamic experiments

The Eqs. (12) and (13) which describe, respectively, the functions $Z(\alpha)$ and $Y(\alpha)$ for dynamic conditions, were applied to the data issued from the dynamic experiments. The resulting curves show the same profile regardless of the heating rate (Fig. 9) and from them the maxima of the functions $Z(\alpha)$ and $Y(\alpha)$ were determined as $\alpha_Z^* = 0.45$ and $\alpha_Y^* = 0.31$, respectively. Thus,

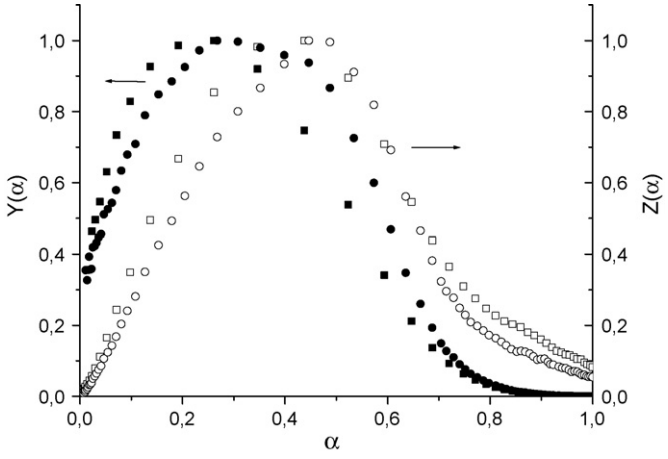

Fig. 9. The functions $Y(\alpha)$ (closed legends) and $Z(\alpha)$ (open legends) for the dynamic degradation of chitosan for the following values of heating rate: $\beta = 2.5$ °C/min (□, ■) and $\beta = 15.0$ °C/min (◯, ●).

Table 6
Values of the kinetic exponents m and n for the non-isothermal degradation of chitosan

β (°C/min)	m	n
2.5	1.23	3.52
5.0	0.89	3.18
10.0	1.50	3.04
15.0	1.60	3.40

the catalytic SB model is also the best fitted kinetic model for the dynamic degradation of chitosan. The exponents m and n, which were calculated from Eqs. (15) and (16) are shown in Table 6.

The simulated and the experimental curves corresponding to the dynamic degradation of chitosan at $\beta = 2.5$ °C/min, 5.0 °C/min, 10 °C/min and 15 °C/min show a good agreement for $\alpha < 0.65$ but they diverge for higher extensions of conversion (Fig. 10), suggesting that thermal reactions following other mechanisms may be occurring.

The parameters m and n are related to the reaction mechanism and they describe, respectively, the acceleration and deceleration of the rate of decomposition with respect to conversion. Thus, they describe the reaction that begins with an acceleration of the degradation rate until a maximum is attained, when an nth order-like deceleration becomes dominant through the reaction completion. However, the forms of the curves $Z(\alpha)$ and $Y(\alpha)$ are not strongly affected for different values of T (isothermal experiment) and β (non-isothermal experiment), and the simulated curves in each case – dα/dt versus α and dα/dT versus α for isothermal and non-isothermal experiments, respectively – have different maxima depending on the parameters m and n. Thus, the influence of these parameters on the simulated curves for the isothermal and dynamic degradation of chitosan was eval-

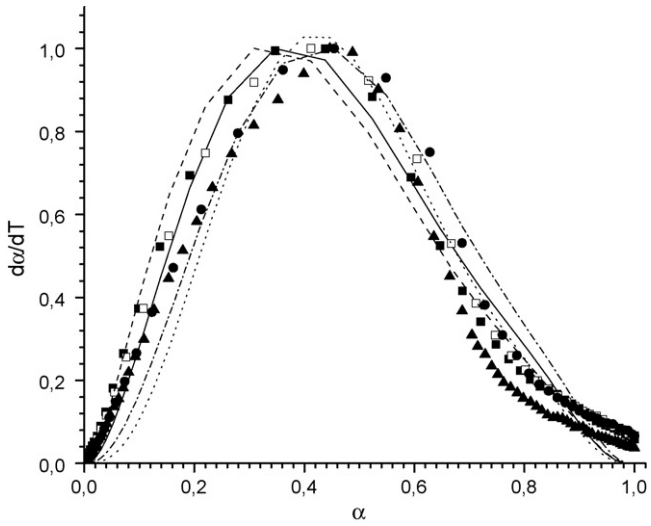

Fig. 10. Experimental (symbols) and simulated (lines) curves dα/dt versus α for the dynamic degradation of chitosan at different $\beta = 2.5$ °C/min (■) experimental/(—) simulated; $\beta = 5.0$ °C/min (□) experimental/(- - -) simulated; $\beta = 10$ °C/min (●) experimental/(· · ·) simulated; $\beta = 15$ °C/min (▲) experimental/(- · - · -) simulated.

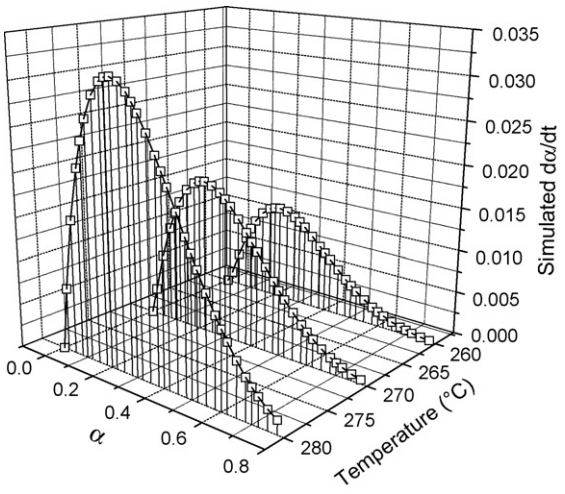

Fig. 11. Plot of simulated dα/dt as a function of α and T for the isothermal degradation of chitosan.

uated (Figs. 11 and 12). From these curves it is observed that dα/dt attains the higher values at high temperatures while higher values of dα/dT are attained at low heating rates.

Concerning the best-fitted kinetics model and reaction mechanism, the most convenient approximation should be [35]:

$$f(\alpha) = \alpha^m(1-\alpha)^n[-\ln(1-\alpha)]^p \quad (17)$$

which combines the three exponents, m, n and p, and a mathematical description of the majority of possible mechanisms. However, the strong inter-correlation of these parameters and the difficulties associated with the numerical solution of Eq. (17) provide only a rough idea of the kinetic model [18,35].

As mentioned before, the FTIR provided some information about the kinetic model. Thus, if the extent of the reaction is expressed as a function of the decrease of the absorbance of a given characteristic band as a function of the reaction time, then:

$$\sigma = \frac{A_0 - A_t}{A_0} \quad (18)$$

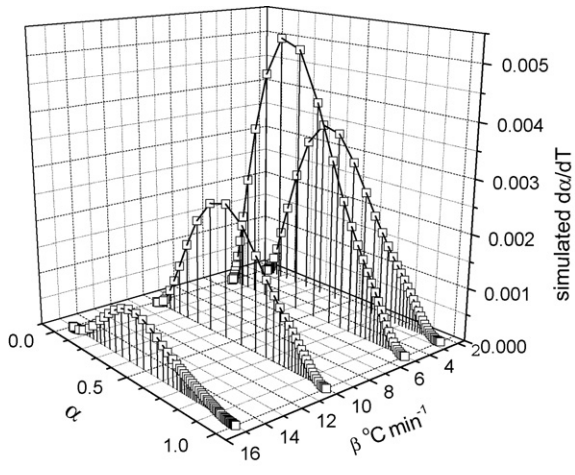

Fig. 12. Plot of simulated dα/dT as a function of α and β for the dynamic degradation of chitosan.

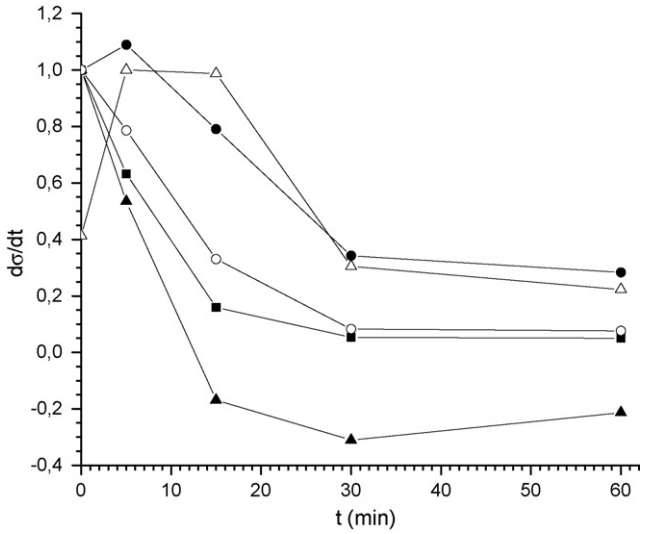

Fig. 13. Plot dσ/dt versus t for infrared bands due to vibrations of O─H (■), C─H (●), C═O (▲), N─H (◯) and glycosidic bond (△).

where σ is the extent of the reaction, A_0 is the absorbance of a given band at zero time and A_t is the absorbance of this same band at time t.

Thus, the best suited degradation model can be investigated by plotting dσ/dt versus t (Fig. 13), showing that the formation of low molecular weight products follows a typical deceleration kinetics model while the scission of the polymer chain is better fitted by a Šesták–Berggren model. Indeed, it is observed that the curves due to the bands O–H (3440 cm^{-1}), C–H (2872 cm^{-1} and 2910 cm^{-1}), C=O (1650 cm^{-1} and 1580 cm^{-1}), C–N (1417 cm^{-1} and 1377 cm^{-1}), which are involved in the decomposition of the hydroxyl and acetamido groups, do not present any maxima. Therefore, these degradation reactions which involve side constituents of the polymer chain and the release of volatile products are better described by a kinetics model of the type $(1-\alpha)^n$ or deceleration.

On the other hand, a maximum is observed in the curve due to the band at 890 cm^{-1} which could be attributed to an acceleratory phase followed by a deacceleratory one. This band is due to the glycosidic bond, responsible for linking together the repeating units of chitosan, and the corresponding curve dσ/dt versus t (Fig. 13) is well described by a Šesták–Berggren model of the type $\alpha^m(1-\alpha)^n$.

From this analysis it is confirmed that during the thermal degradation of chitosan several reactions occur simultaneously and as they follow their own pathways, a single kinetics model may not well describe the whole process.

4.4. The mechanism of degradation

The investigation on the best-suited kinetic model is not an easy task, and the evaluation of the most probable mechanism of degradation is also difficult. According to Sesták [35], the values of m and n can give some insight on the possible mechanism of degradation. Thus, for $m < 1$ and $n > 1$ the process is controlled by nucleation, however this mechanism seldom occurs during the degradation of polymers.

The Coats–Redfern equation [36] is a very popular method to evaluate the Arrhenius parameters as well as the kinetic models and the mechanism of the degradation process. This method is known as the model fitting approach [18] and by applying it the parameters E_a and A are calculated by testing different kinetic models, $g(\alpha)$. As discussed by Galwey [37], the most important critics to this method are: (i) the parameters E_a and A are highly variable, exhibiting a strong dependence on the reaction model chosen; (ii) the impossibility to choose a kinetic model once, generally, the values of r issued from different models are only slightly different and (iii) it is based in a single non-isothermal experiment, giving information about $g(\alpha)$ and the parameters E_a and A, but not independently.

Despite of the limitations mentioned above, some authors use to determine the Arrhenius parameters (E_a and A) by applying more elaborated methods, such as Ozawa–Flynn–Wall's and Vyazovkin's approaches, and to validate their kinetic model by comparing it to that one issued from the application of the Coats–Redfern method [30,31,38,39]. By applying the Coats–Redfern approach to the non-isothermal data of the thermal degradation of chitosan at $\beta = 10\,^{\circ}$C/min, it is found that the better agreements in terms of the apparent activation energy were found for a phase-boundary-controlled reaction (contracting sphere or cylinder) and the random nucleation (Mampel first order).

From the discussions presented here, it is clear that further investigation on the kinetics of the thermal degradation of chitosan is necessary. In this sense, coupling the thermal degradation analysis with mass spectrometry and infrared spectroscopy would greatly contribute to elucidate the reaction mechanisms.

5. Conclusions

The apparent activation energy of the thermal degradation of chitosan is independent of the method, isothermal or dynamic, used for its determination but the effect of the average degree of acetylation and physical form of the polymer as well as of the atmosphere employed to study the degradation of the polymer should be investigated. Also, the thermal degradation of chitosan, in isothermal as well as in dynamic conditions, seems to be well described by the catalytic Šesták–Berggren model, however further studies should be carried out to investigate the role of the experimental conditions and to elucidate the reaction mechanism.

Work is in progress to evaluate the influence of the physical form, average degree of acetylation and counter ion of chitosan salts in its thermal degradation.

Acknowledgments

The authors are grateful to FAPESP and CNPq for financial support.

References

[1] G.A.F. Roberts, Chitin Chemistry, Macmillan Press, London/UK, 1992.
[2] R.A.A. Muzzarelli, Carbohydr. Polym. 29 (1996) 309–316.
[3] P. Vander, K.M. Vårum, A. Domard, N.E. El Geddari, B. Moerschbacher, Plant Physiol. 118 (1998) 1353–1359.
[4] G. Peluso, O. Petillo, M. Ranieri, M. Santin, L. Ambrosio, D. Calabro, B. Avallone, G. Balsamo, Biomaterials 15 (1994) 1215–1220.
[5] P. Gérentes, L. Vachoud, J. Doury, A. Domard, Biomaterials 23 (2002) 1295–1302.
[6] S. Despond, E. Espuche, A. Domard, J. Polym. Sci. Part B 39 (2001) 3114–3127.
[7] G. Kumar, J.F. Bristow, P.J. Smith, G.F. Payne, Polymer 41 (2000) 2157–2168.
[8] H.K. Holme, H. Foros, H. Pettersen, M. Dornish, O. Smidsrød, Carbohydr. Polym. 46 (2001) 287–294.
[9] U. Piotr, S. von Clemens, J. Chem. Soc. Perkin Trans. 2 (2000) 2022–2028.
[10] W.S. Choi, K.J. Ahn, D.W. Lee, M.W. Byun, H.J. Park, Polym. Degrad. Stab. 78 (2002) 533–538.
[11] J. Shao, Y. Yang, Q. Zhong, Polym. Degrad. Stab. 82 (2003) 395–398.
[12] G.T. Cárdenas, L.A. Bernal, L.H.D. Tagle, Termochim. Acta 195 (1992) 33–38.
[13] C. Peniche-Covas, W. Monal-Argüelles, J.S. Román, Polym. Degrad. Stab. 39 (1993) 21–28.
[14] X. Qu, A. Wirsén, A.-C. Albertsson, Polymer 41 (2000) 4841–4847.
[15] A. Pawlak, M. Mucha, Termochim. Acta 396 (2003) 153–166.
[16] D. Britto, S.P. Campana-Filho, Polym. Degrad. Stab. 84 (2004) 353–361.
[17] J. Málek, J. Šesták, F. Rouquerol, J.M. Criado, A. Ortega, J. Therm. Anal. 38 (1992) 71–87.
[18] S. Vyazovkin, C.A. Wight, Int. Rev. Phys. Chem. 17 (1998) 407–433.
[19] J.R. MacCallum, in: C. Booth, C. Price (Eds.), Thermogravimetric Analysis, vol. 1, Pergamon Press, Oxford, 1989, pp. 903–909.
[20] J.H. Flynn, Thermochim. Acta 300 (1997) 83–92.
[21] T. Ozawa, J. Therm. Anal. 2 (1970) 301.
[22] C. Doyle, J. Appl. Polym. Sci. 6 (1962) 639.
[23] L.S. Guinesi, C.A. Ribeiro, M.S. Crespi, A.M. Veronezi, Termochim. Acta 414 (2004) 35–42.
[24] H.E. Kinssinger, Anal. Chem. 29 (1957) 1702.
[25] S. Montserrat, J. Málek, P. Colomer, Termochim. Acta 313 (1998) 83–95.
[26] A. Hirai, H. Odani, A. Nkajima, Polym. Bull. 26 (1991) 87–94.
[27] B. Focher, P.L. Beltrame, A. Naggi, G. Torri, Carbohydr. Polym. 12 (1990) 405.
[28] B. Focher, A. Naggi, G. Torri, A. Cosani, M. Terbojevich, Carbohydr. Polym. 18 (1992) 43.
[29] S. Vyazovkin, D. Dollimore, J. Chem. Inf. Comput. Sci. 36 (1996) 42.
[30] A. Khawam, D.R. Flanagan, Termochim. Acta 436 (2005) 101–112.
[31] X. Fernandez, X. Ramis, J.M. Salla, Termochim. Acta 438 (2005) 144–154.
[32] A. Broido, J. Polym. Sci. Part A-2 7 (1969) 1761–1773.
[33] P.Z. Hong, S.D. Li, C.Y. Ou, C.P. Li, L. Yang, C.H. Zhang, J. Appl. Polym. Sci. 105 (2007) 547–551.
[34] Z. Gao, I. Amasaki, T. Kaneko, M. Nakada, Polym. Degrad. Stab. 83 (2004) 67–70.
[35] J. Šesták, Termochim. Acta 3 (1971) 1–12.
[36] A.W. Coats, J.P. Redfern, Nature 207 (1965) 209.
[37] A.K. Galwey, Termochim. Acta 399 (2003) 1–29.
[38] B. Liu, X. Zhao, X. Wang, F. Wang, J. Appl. Polym. Sci. 90 (2003) 947–953.
[39] F. Fraga, Rodriguez-Nuñez, J. Appl. Polym. Sci. 80 (2001) 776–782.